

# Critical and Non-Critical Avalanche Behavior in Networks of Integrate-and-Fire Neurons

Christian W. Eurich\*, Thorsten Conradi and Helmut Schwegler

Institut für Theoretische Physik, Universität Bremen  
Kufsteiner Str., D-28359 Bremen, Germany

**Abstract.** We study avalanches of spike activity in fully connected networks of integrate-and-fire neurons which receive purely random input. In contrast to the self-organized critical avalanche behavior in sandpile models, critical and non-critical behavior is found depending on the interaction strength. Avalanche behavior can be readily understood by using combinatorial arguments in phase space.

## 1. Introduction

The dynamics of networks of interacting threshold elements have focused much attention in the last years. Single elements are characterized by an internal variable,  $U$ , which accumulates as the element receives external or internal input. Upon reaching a threshold,  $U_{\max}$ , the element interacts with other members of the network, and  $U$  is reset. Phenomena arising in such networks range from partial and total synchronization and desynchronization (e. g. [8, 5, 9]) to self-organized criticality (SOC; e. g. [1, 7, 10, 11]).

Self-organized criticality was introduced by Bak et al. [1, 2] in the context of cellular automata – finite-state systems with nearest-neighbor coupling – which are driven by random input (sandpile model). The size and temporal duration of avalanches of activity in such systems have power-law distributions. SOC has recently been characterized by an infinite separation of the time scales of external driving (which is slow) and avalanche dynamics (which is fast) [11]. Feder and Feder [7] and Olami et al. [10] studied the avalanche behavior of a different type of systems exhibiting SOC, the so-called stick-slip models which are nonconservative cellular automata with a uniform instead of a random driving. The collective behavior of integrate-and-fire neural networks with different topologies has been intensively investigated under various conditions (e. g., [8, 4, 3, 5, 9]). In these models, the external input is usually assumed to be uniform, and the system is studied with respect to the question under which conditions synchronized and desynchronized states occur.

---

\*e-mail: eurich@physik.uni-bremen.de

In the present study we focus attention on avalanches in randomly driven systems with an infinite separation of time scales. Instead of a nearest-neighbor coupling as in cellular automata, however, we consider networks of integrate-and-fire neurons with global coupling. Compared to the sandpile model [1, 2], additional parameters are introduced: the size of the synaptic weights and the size of the external input. Accordingly, a behavior richer than pure SOC can be expected.

## 2. Model

Time is measured in discrete steps,  $t = 0, 1, 2, \dots$ . The network consists of  $N$  identical perfect integrate-and-fire neurons with uniform all-to-all coupling. The state of each neuron is described by the membrane potential,  $U \in [0; U_{\max}]$ , where  $U_{\max}$  is the firing threshold. For the  $i$ -th neuron ( $i = 1, \dots, N$ ), the dynamics are governed by the equation

$$U_i(t+1) = (U_i(t) + I_i^{\text{int}}(t) + I_i^{\text{ext}}(t)) \bmod U_{\max}, \quad (1)$$

where  $I_i^{\text{int}}(t)$  represents the internal and  $I_i^{\text{ext}}(t)$  the external input at time  $t$ . Equation (1) corresponds to a fast relaxation of the membrane potential after having reached the threshold such that the excess input,  $U_i(t) + I_i^{\text{int}}(t) + I_i^{\text{ext}}(t) - U_{\max}$ , is accumulated after the reset [9]. The internal input is given by  $I_i^{\text{int}}(t) = M(t-1)\alpha/N$ , where  $M(t-1)$  is the number of neurons having fired at time  $t-1$ , and  $\alpha/N$  is the synaptic weight. We assume  $\alpha \geq 0$  (excitatory input) and  $\alpha < U_{\max}$  for simplicity. For the external input, one neuron is randomly chosen from the network according to a uniform distribution, and a constant  $0 \leq \Delta U \leq U_{\max}$  is added to its potential. The external input is considered to be delivered slowly compared to the internal network dynamics, i. e., it occurs only after neural firing has ceased. This can be written as  $I_i^{\text{ext}}(t) = \delta_{ri} \delta_{M(t-1)0} \Delta U$ , where  $r$  is an integer random variable between 1 and  $N$ .

At some time  $t_0$  an avalanche starts if the neuron receiving external input fires, i.e.,  $M(t_0) = 1$ . During the avalanche, there is no external input. Spikes are transmitted to all neurons (including the neurons which have fired). The stopping condition for an avalanche is  $M(t_0 + t_L) = 0$ , where  $t_L$  is defined to be the avalanche duration. The avalanche size,  $L$ , is defined to be  $L = \sum_{k=0}^{t_L-1} M(t_0 + k)$  and the relative avalanche size is  $l = L/N$ . Avalanche distributions are described either by a function  $p(l)$  where  $\sum_{l \geq 1/N} p(l) = 1$ , or by a function  $P(L)$  where  $\sum_{L \geq 0} P(L) = 1$ . Both measures are related to each other via  $p(L/N) = P(L)/(1 - P(0))$ .

## 3. Results

Figure 1 shows double-logarithmic plots of avalanche distributions,  $p(l)$ , for different values of the coupling strength  $\alpha$  while  $N$  and  $\Delta U$  are held fixed. In general, four qualitatively different avalanche behaviors exist which will be

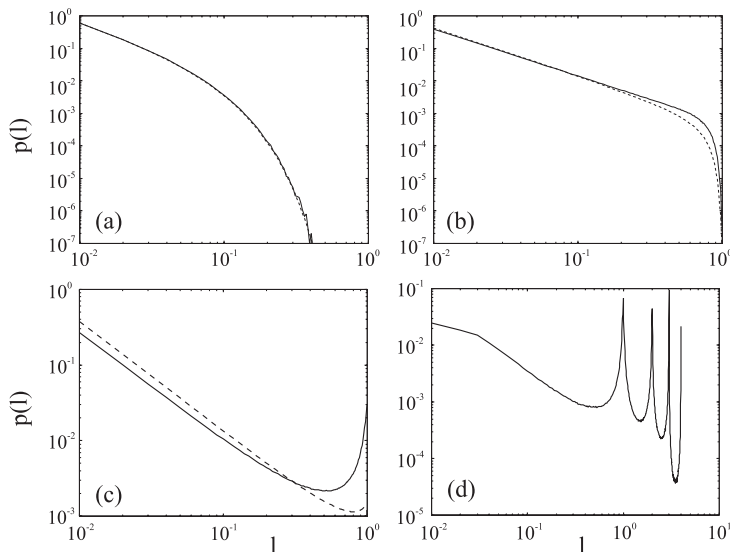


Figure 1: Distributions of avalanche sizes,  $p(l)$ , in the subcritical (a;  $\alpha = 0.503$ ), critical (b;  $\alpha = 0.874$ ), supercritical (c;  $\alpha = 0.977$ ) and hypercritical (d;  $\alpha = 0.997$ ) regime. Solid lines: numerical results. Dashed lines in a)–c): Analytical results. In all cases,  $N = 100$ ,  $\Delta U = 0.022$ ,  $U_{\max} = 1$ . Temporal average over  $10^7$  avalanches.

called subcritical, critical, supercritical and hypercritical, respectively. Figure 1a shows an example of the subcritical case. The curve is monotonically decreasing and concave down. Typically, the probability of global avalanches comprising a high percentage of neurons in the network is so low that they are not found numerically. As  $\alpha$  is increased, the critical case is eventually reached (Fig. 1b). The critical regime was found numerically to satisfy approximately  $\alpha(N) = 1 - N^{-0.45}$ . Avalanche distributions show power-law behavior which holds from  $L = 1$  almost up to  $L = N + 1$ . Deviations result from the finite size of the network. Numerical calculations yield  $p(l) \approx l^{-1.45}$  independent of  $N$  and  $\Delta U$ . Above the critical value of  $\alpha$ , avalanche size distributions become nonmonotonic (Fig. 1c). The supercritical curves have a minimum at some intermediate avalanche size: large avalanches are more probable than medium-sized ones. This phenomenon could be termed “stochastic synchronicity”: the system tends to show outbreaks of high activity comprising the firing of a majority of elements. Finally, for values of  $\alpha$  close to  $U_{\max}$ , neurons can fire more than once during an avalanche leading to distributions which have multiple peaks for values  $l = 1, 2, 3, \dots$ . Figure 1d shows an example with four peaks. A simple geometric argument reveals that avalanches of size  $L = N + 1$  can only occur if  $\alpha + \Delta U > U_{\max}$ . For the existence of  $k$  peaks in the avalanche distri-

bution, the condition  $\alpha > (kNU_{\max})/(kN + 1)$  has to be satisfied in addition [6].

In the following, we use combinatorial arguments in phase space to derive expressions for avalanche distributions. The phase space of the system is given by the Cartesian product  $\Pi = \mathbb{N}^0 \times \pi$  where the first factor describes the temporal dimension, and  $\pi = [0; U_{\max}]^N$  is the space of the neurons' membrane potentials.

First consider the case  $N = 2$  which demonstrates the basic mechanisms for evaluating the avalanche dynamics. The avalanche distribution is calculated by determining the equilibrium density of states in  $\pi$ ,  $\rho(U_1, U_2)$ , and subsequently considering the subspaces which lead to avalanches of sizes 0, 1, and 2. Figure 2a shows the subspace  $\pi$  and the effects of external input, internal input, and an avalanche of size  $L = 1$ . In the latter case, the system leaves  $\pi$  and is reinjected on the opposite side. Considering the long time scale between avalanches, it is straightforward to see that systems will never be reinjected into the subspace denoted as  $A$ , i.e.,  $\rho(U_1, U_2) = 0$  for  $(U_1, U_2) \in A$ . The density in  $\pi \setminus A$  is solely determined by the external input the random nature of which results in a random walk along the second diagonal while the system makes deterministic steps of size  $\sqrt{2}\Delta U$  along the first diagonal. As a result, the density is constant in  $\pi \setminus A$ , and a normalization yields the value  $\rho(U_1, U_2) = (U_{\max}^2 - \alpha U_{\max})^{-1}$  in  $\pi \setminus A$ . Figure 2b identifies those regions in phase space which lead to avalanches of size 0 ( $B$ ), 1 ( $C$ ), and 2 ( $D$ ) following external input to neuron 1. Avalanche probabilities are obtained by integrating  $\rho(U_1, U_2)$  over the respective region. The result is  $P(L = 1) = \Delta U/U_{\max}$ ;  $P(L = 2) = \alpha\Delta U/(2U_{\max}^2 - \alpha U_{\max})$ .

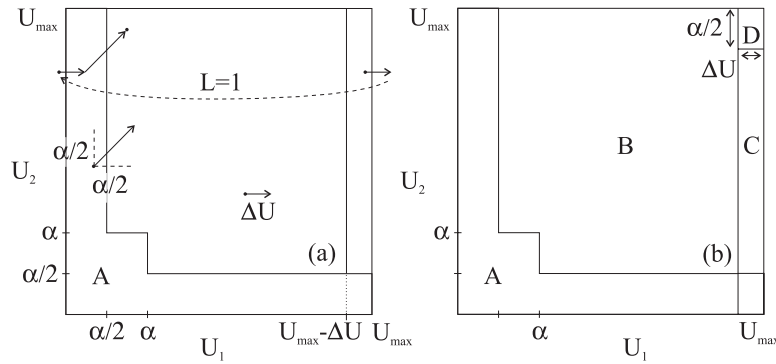


Figure 2: The dynamics in the subspace  $\pi$  for  $N = 2$ . (a) Effects of an external input to neuron 1 (arrow marked as  $\Delta U$ ), internal input (arrow marked as  $\alpha/2$ ), and an avalanche of size 1 (arrows marked as  $L = 1$ ).  $A$  denotes the subspace where the density of states eventually vanishes. (b)  $B, C, D$  denote subspaces leading to avalanches of size  $L = 0, 1, 2$ , respectively, if triggered by an external input to neuron 1.

Similar arguments hold for the general situation of  $N$  neurons; the topology

of the subspace  $A$  and the subspaces leading to avalanches of certain sizes, however, are more complicated. An analytical expression can be obtained for  $\alpha \rightarrow 0$  which allows the use of a combinatorial argument in  $\pi$  instead of  $\pi \setminus A$ . For this purpose, the set of membrane potentials of a neuron,  $[0; U_{\max}[$ , is divided into intervals  $I_i$  where  $I_i \equiv [U_{\max} - i \frac{\alpha}{N}; U_{\max} - (i-1) \frac{\alpha}{N}[$  ( $i = 1, \dots, N$ ). Furthermore, let  $I_0 \equiv [U_{\max} - \Delta U; U_{\max}[$  and  $\text{Vol}(L; N, \alpha) = P(L)$  denote the volume of the subspace containing all regions which result in avalanches of size  $L$ . For  $L = 0$ , no membrane potential must be closer to the threshold than  $\Delta U$ . The corresponding volume in  $\pi$  is  $\text{Vol}(0; N, \alpha) = (U_{\max} - \Delta U) U_{\max}^{N-1}$ . For avalanches of size  $L \geq 1$ , neuron 1 which receives external input fires.<sup>1</sup> For  $L = 1$ , it is required that neuron 1 be in  $I_0$  while no other neuron must be in  $I_1$ . This yields a volume  $\text{Vol}(1; N, \alpha) = \Delta U (U_{\max} - \frac{\alpha}{N})^{N-1}$ . Phase space volumes for larger avalanches are calculated accordingly; for  $L \geq 3$ , however, two facts have to be taken into account: First, two or more neurons in the same interval  $I_i$  are indistinguishable. Second, there are several configurations leading to the same avalanche size [6]. A tedious calculation of the cases  $L = 1, \dots, 10$  suggests the general formula

$$\text{Vol}(L; N, \alpha) = C(N, L) \Delta U \left(\frac{\alpha}{N}\right)^{L-1} \left(U_{\max} - \frac{L\alpha}{N}\right)^{N-L}, \quad (2)$$

where

$$C(N, L) = \frac{L^{L-2} (N-1)!}{(L-1)! (N-L)!} = L^{L-2} \binom{N-1}{L-1}. \quad (3)$$

The dashed lines in Fig. 1a-c show  $p(l)$  as evaluated by (2) and (3). In the subcritical case, the approximation yields very good results even if  $\alpha$  is not close to zero. The critical case shows a quantitative agreement of numerical and analytical calculations for small avalanche sizes. Especially, the power-law behavior is obtained from the approximation. In the supercritical case, the nonmonotonic character of the distribution is recovered. This is true although  $\alpha$  is close to one rather than close to zero.

## 4. Summary and Discussion

We studied the avalanche behavior in fully connected networks of perfect integrate-and-fire neurons with random input. Depending on the strength of interaction between the neurons,  $\alpha$ , four qualitative different avalanche distributions were obtained which we termed subcritical, critical, supercritical, and hypercritical.

The avalanche behavior of the fully connected network differs from the avalanche behavior of the classical sandpile model [1, 2] with respect to two properties. First, in our model, the regimes of the four different types of avalanche distributions depend on  $N$  while the avalanche distribution of the

<sup>1</sup>More specifically, all  $N$  neurons are considered and yield identical results; these are weighted by the probability,  $1/N$ , of choosing the respective neuron.

sandpile model is independent of the size of the system. This is due to the different network topologies: in the sandpile model, each neuron is connected to a fixed number of neighbors irrespective of the system size. In the fully connected network, however, each neuron receives input from  $\mathcal{O}(N)$  neurons which alters the statistical properties as a function of  $N$ . In fact, the critical, supercritical and hypercritical behaviors live on the statistical fluctuations of the distribution of membrane potentials which are most prominent for small numbers of neurons. Second, in the fully connected network, the critical state which is characterized by a power-law distribution of avalanche sizes requires a fine-tuning of the coupling constant in addition to the infinite separation of the time scales of external driving and avalanche dynamics employed in the sandpile model [1, 2, 11]. In this sense, our system is more general than the sandpile model in that we introduced additional parameters part of which then have to be tuned to certain values in order to obtain self-similar behavior.

Extensions of the current model include the consideration of various network topologies such as a two-dimensional array of neurons whose coupling constants fall off with distance, and the study of the transition from perfect integrate-and-fire neurons to leaky integrators. In the latter project, the prerequisite of the infinite separation of time scales has to be dropped. Both extensions aim at greater biological plausibility in order to assess the question if avalanche phenomena arise in the brain, e.g., in neocortical structures with its diffuse thalamic and reticular input.

## References

- [1] P. Bak, C. Tang, and K. Wiesenfeld. *Phys. Rev. Lett.*, 59:381–384, 1987.
- [2] P. Bak, C. Tang, and K. Wiesenfeld. *Phys. Rev. A*, 38:364–374, 1988.
- [3] S. Bottani. *Phys. Rev. Lett.*, 74:4189–4192, 1995.
- [4] A. Corral, C. J. Pérez, A. Díaz-Guilera, and A. Arenas. *Phys. Rev. Lett.*, 74:118–121, 1995.
- [5] U. Ernst, K. Pawelzik, and T. Geisel. *Phys. Rev. Lett.*, 74:1570–1573, 1995.
- [6] C. W. Eurich, T. Conradi, and H. Schwegler. Submitted to *Physica D*.
- [7] H. J. S. Feder and J. Feder. *Phys. Rev. Lett.*, 66:2669–2672, 1991.
- [8] W. Gerstner and J. L. van Hemmen. *Phys. Rev. Lett.*, 71:312–315, 1993.
- [9] A. V. M. Herz and J. J. Hopfield. *Phys. Rev. Lett.*, 75:1222–1225, 1995.
- [10] Z. Olami, H. J. S. Feder, and K. Christensen. *Phys. Rev. Lett.*, 68:1244–1247, 1992.
- [11] D. Sornette, A. Johnansen, and I. Dornic. *J. Phys. I*, 5:325–335, 1995.